16 November 2001

ELSEVIER

Chemical Physics Letters 348 (2001) 368–374

CHEMICAL PHYSICS LETTERS

www.elsevier.com/locate/cplett

Multilayered metal catalysts for controlling the density of single-walled carbon nanotube growth

Lance Delzeit [a,*], Bin Chen [b], Alan Cassell [b], Ramsey Stevens [b], Cattien Nguyen [b], M. Meyyappan [a]

[a] *NASA Ames Research Center, MS 239-4, Moffett Field, CA 94035, USA*
[b] *Eloret Corporation, 690 W. Fremont Ave, Suite 8, Sunnyvale, CA 94087-4202, USA*

Received 6 August 2001; in final form 29 August 2001

Abstract

Ion beam sputtering has been used for the sequential deposition of metal multilayers on various substrates to control the density of single-walled carbon nanotubes (SWNTs) synthesized by chemical vapor deposition. Underlayers (10–20 nm) of Al and Ir were found to activate the substrates for SWNT growth with Fe as active catalyst. Adding Mo as co-catalyst gives increased production of SWNTs and the density can be controlled by varying the thickness of the different metal layers. High-resolution transmission electron microscopy and Raman scattering are used to characterize the SWNTs.

1. Introduction

Carbon nanotubes (CNTs) exhibit extraordinary mechanical and unique electronic properties and hence have been receiving much attention in recent years for their potential in nanoelectronics, field emission devices, scanning probes, high strength composites and many more applications. In the early years of CNT research, the primary approaches to produce nanotubes consisted of laser vaporization [1] and arc-evaporation of graphite electrodes [2]. More recently, catalytic decomposition of hydrocarbon or CO feedstock with the aid of supported transition metal catalysts – also known as chemical vapor deposition (CVD) – has become popular to produce both single-walled and multiwalled nanotubes (SWNTs, MWNTs) [3–14]. The ability to grow nanotubes on patterned substrates and in vertically aligned arrays and the simplicity of the process have made CVD an attractive approach [7,11]. A variation of this without supported catalysts but relying on gas phase pyrolysis [15] or CO disproportionation [16] has also been proposed.

The choices for the catalyst, substrate, and the method to transfer the catalyst to the substrate are critical to the success of CVD of nanotubes. Typically, the catalyst precursor and structure directing agents or other additives, if any, are in a solution which is evaporated and calcined to prepare the catalyst formulation on the substrate [7–10]. Chen et al. [5] used a Ni–MgO catalyst in methane decomposition to produce MWNTs and

* Corresponding author. Fax: +1-650-604-5244.
E-mail address: ldelzeit@mail.arc.nasa.gov (L. Delzeit).

0009-2614/01/$ - see front matter
PII: S0009-2614(01)01148-4

their experiments indicated that the rate determining step in nanotube growth depended on the feedgas and its flow rate as well as temperature. Pan et al. [6] used a sol–gel process involving tetraethoxysilane, aqueous solution of iron nitrate and ethyl alcohol to prepare a porous catalyst that produced very long (up to 2 mm) MWNTs from a flow of 9% acetylene in nitrogen. Kind et al. [8] adopted a micro-contact printing to transfer iron-containing gel-like catalysts from a hydrophilized elastomeric stamp to the substrate and demonstrated MWNT growth from acetylene. Their study suggested that numerous factors such as the catalyst, nature and concentration of ink, annealing time, substrate material, and temperature have impact on the outcome of CVD. Recognizing the large parametric space, Cassell et al. [9] introduced a high throughput combinatorial optimization technique for catalyst development and successfully used it to grow ~100 μm tall MWNT towers. This process was also used in multilayer assembly of CNTs [10]. Solution-based catalyst preparation is often found to produce only MWNTs with the exception of [7,13,14]. Another notable problem with the various solution-based catalyst preparation techniques discussed above is the difficulty in confining the catalyst within patterns, particularly in small feature sizes needed for device development. In this regard, nanochannel alumina templates made by anodization have been helpful in growing highly ordered arrays of MWNTs [11]. Various physical deposition approaches have also been used to apply the catalyst to the surface including electron-gun evaporation [12] and magnetron sputtering [17], though these also produced only MWNTs. In this Letter, we report preparation of thin catalyst films by ion beam sputtering and growth of SWNTs on a variety of patterned and unpatterned substrates.

2. Experimental

Our approach uses ion beam sputtering for the deposition of the metal catalyst to grow SWNTs. The metals used in these experiments are 99.9+% pure and are sputtered using a VCR Group Incorporated Ion Beam Sputterer, model IBS/TM200s. The catalyst used to grow the SWNTs consists of two components: a metal underlayer and an active catalyst. The candidate materials for the underlayer includes Ir, Al, Nb, and Ti and the thickness of the metal underlayer is varied from 1 to 20 nm. The metal used as active catalyst is Fe. Mo is also added to the Fe in some trials in order to modify the density of the SWNTs.

We have studied a variety of substrates such as Si wafers, Si atomic force microscope (AFM) cantilevers, fused quartz, mica, amorphous carbon and highly oriented pyrolytic graphite (HOPG). The substrate with the catalyst formulation is then inserted into the CVD reactor which consists of a quartz tube within a high temperature furnace and mass flow controllers [9]. Argon (Scott Specialty Gases, 99.999% pure) flow (1000 sccm) is used to purge the reactor while the furnace is heated to 900 °C. After the furnace reaches 900 °C, it is allowed an additional 5 min for the temperature to equilibrate. The gas flow is then switched to 1000 sccm of methane (Scott Specialty Gases, 99.999% pure), for 10 min. The gas flow is switched back to argon after the growth process to purge the methane from the tube and to prevent back flow of air into the tube. The furnace is then allowed to cool below 300 °C before exposing the NTs to air. Exposure to air at elevated temperatures can cause damage to the NTs.

3. Results and discussion

We first investigated thin layers of iron on various substrates. No SWNTs were grown with 0.1–1.0 nm Fe on smooth clean substrates. However, if there are scratches or other small particles on the substrate, then a few SWNTs were found growing off these structures (Fig. 1a). This level of SWNT growth for most applications would be highly unsatisfactory; however, it does show the lower limit of the growth possibilities. Next, an Ir underlayer was added to increase the surface roughness and provide more active nucleation sites, and the effect of varying its thickness was investigated with Fe layer thickness fixed at 1 nm. A 5 nm thick underlayer of Ir did not promote the growth of the SWNTs; however a 20 nm under-

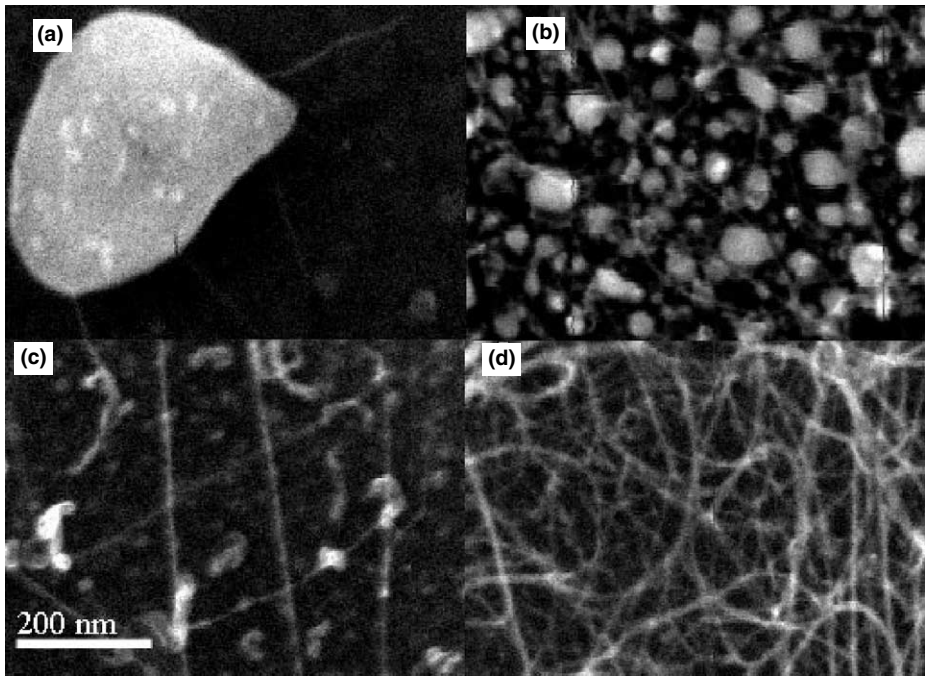

Fig. 1. SEM images of SWNTs on a silicon substrate showing a range of possible densities that can be grown. The active catalyst is 1.0 nm Fe deposited onto an underlayer of (a) 0 nm (b) 20 nm Ir, (c) 1 nm Al, and (d) 10 nm Al. Cases (c) and (d) also have 0.2 nm Mo as co-catalyst. The tubes seen in (a) and (b) are individual SWNTs, while the tubes seen in (c) and (d) are SWNT ropes.

layer of Ir did increase the density of the SWNTs (Fig. 1b). Increasing the Ir thickness further to 40 nm did not enhance the yield of SWNTs. It is important to note that a 1 nm active catalyst layer (Fe) is adequate to produce nanotubes with the addition of an underlayer such as Ir. Previous work on CVD of MWNTs [10] clearly showed that nucleation and growth of nanotubes increase with a decrease in catalyst layer thickness at a fixed growth temperature.

A thin layer of Mo as co-catalyst was also added to the formula and did produce a slight increase in the density of the SWNTs grown. However, if the Ir underlayer is not used, then the Mo has no effect and there are no SWNTs grown. Several other metals (Al, Nb, and Ti) were also tried as the underlayer. Of these, only Al increased the production of SWNTs and Nb and Ti were not useful. In fact, the quantity of SWNTs produced with the Al underlayer was much greater than that with Ir underlayer and therefore, optimization of Al underlayers was also undertaken. The thickness of the Al underlayer was then varied and found that the density of the SWNTs grown increases with an increase in Al underlayer thickness from 1 to 10 nm (Fig. 1c, d). Increasing the thickness of the Al underlayer beyond 10 nm does not produce a noticeable increase in the density of the SWNTs. Varying the Mo thickness yielded best results (in terms of density) with 0.2 nm of Mo. These results demonstrate that the density of the SWNTs can be controlled from sparse distribution of individual tubes to thick mats of SWNTs ropes, as shown in Fig. 1.

Fig. 2 shows TEM results confirming that the nanotubes grown are in fact SWNTs. Fig. 2a shows two individual SWNTs grown with 20 nm Ir/1.0 nm Fe/0.2 nm Mo from the tip of an AFM cantilever. Notice how the two individual SWNTs are coming together, the start of rope formation. Fig. 2b shows a thick mat of SWNT ropes grown on a silicon substrate using a 10 nm Al/1.0 nm Fe/0.2 nm Mo formulation. The diameter range is estimated to be 0.9–2.7 nm with most tubes at 1.3 nm. Of a

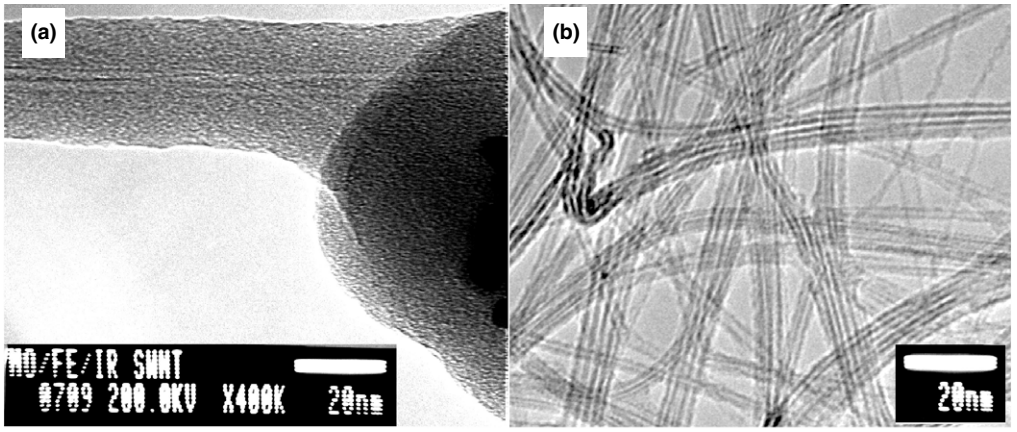

Fig. 2. TEM of (a) two individual SWNTs growing off of the end of an AFM cantilever prepared from a 20 nm Ir/1.0 nm Fe/0.2 nm Mo catalyst formulation and (b) a dense mat of SWNT ropes grown from a 10 nm Al/1.0 nm Fe/0.2 nm Mo catalyst formulation on silicon. The amorphous carbon in (a) is not from growth but deposited within TEM.

total count of 48 tubes, the diameter distribution is found to be (in nanometers) 0.9 (10%), 1.3 (44%), 1.8 (29%), 2.2 (10%), and 2.7 (6%).

The above observations are also consistent with Raman analysis. Raman spectra were obtained with System 2000 micro-Raman spectrometer (Renishaw Product) in the back scattering configuration. We used 2 mW laser power on the sample with 1 μm focus spot. 514 and 633 nm excitation lasers were employed to achieve metallic and semiconducting nanotube resonance Raman enhancement. Spectra were taken at least in three different spots to ensure the reproducibility for peak intensities. As extensively studied before, nanotube G band zone is formed through graphite Brillouin zone folding. According to group theory, the tangential mode (TM) exhibits A_1, E_1 and E_2 symmetry that are Raman active [18]. Our sample Raman spectrum (Fig. 3) shows the characteristic narrow G band at 1590 cm^{-1} and signature band at 1730 cm^{-1} as single wall CNTs. We also observed the strong enhancement in the low frequency region for the radial breathing mode (RBM) from 633 nm laser excitation. As shown in

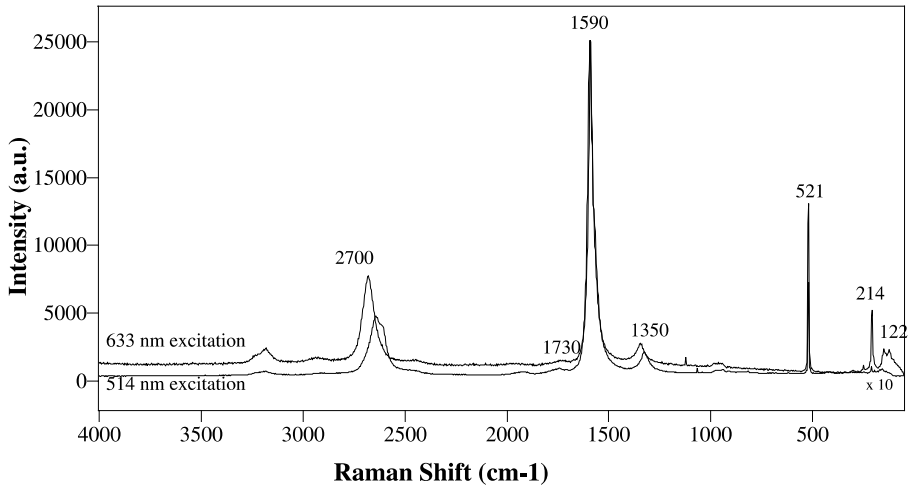

Fig. 3. Raman spectrum of the CNTs.

previous studies [19], one-dimensional density of state of metallic nanotube near Fermi level has the first singularity band gap between 1.7 and 2.2 eV, which will be resonant with 633 nm (1.96 eV) excitation line to the RBM. The excitation shift from 514 to 633 nm is probably due to the coupling between conduction electron and phonon. We used $\alpha = 248\ \mathrm{cm}^{-1}$ in the equation $\Omega_{\mathrm{RBM}}\ (\mathrm{cm}^{-1}) = \alpha/d\ (\mathrm{nm})$ to estimate the nanotube diameter [20]. Clearly, we have a very broad diameter distribution in the sample ranging from 1.14 to 2 nm as shown in Fig. 3, with dominant distribution around 1.16 nm. The smaller diameter nanotube sample is resonant enhanced with excitation of 633 nm which indicates that different diameter ensembles couple the frequency mode with laser field with different efficiencies. The strong enhancement in 633 nm excitation [21] shows that our sample preferentially consists of metallic nanotubes. We do recognize the fact that the Breit–Wigner–Fano line shape is missing for the metallic nanotubes which, we believe, is related to the bundle effect [22]. Our curve fit results show the tangential G band in this diameter region with both 633 and 514 nm excitations include A and E_1 modes (at 1595 and 590.9 cm^{-1}, respectively), as well as E_2 mode (at 1548.4 and 1545 cm^{-1}, respectively) [19,20]. The central graphite frequency 1586 cm^{-1} is very substantial in the 633 nm laser excitation, another indication of high metallic percentage of nanotubes in the sample [21].

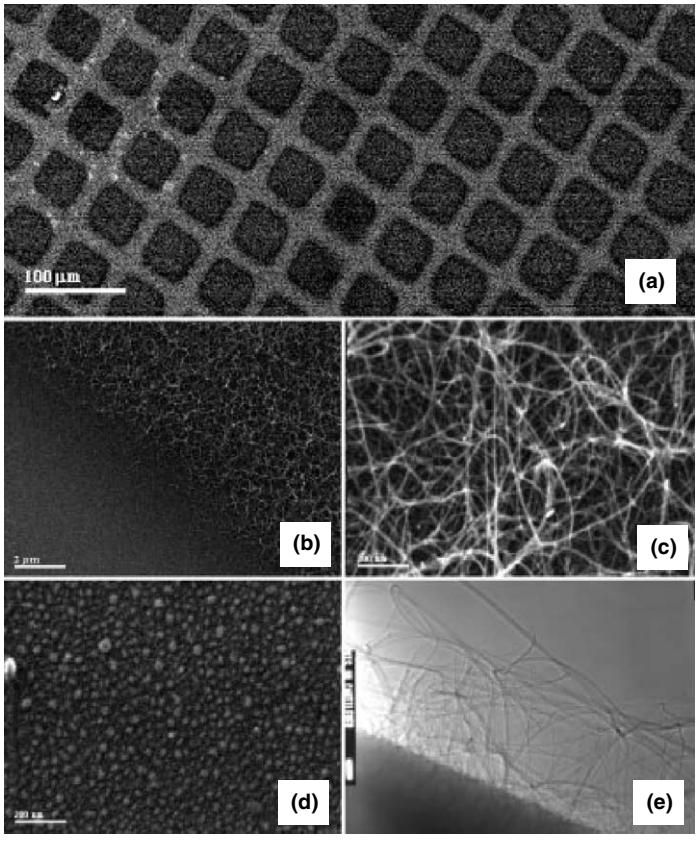

Fig. 4. (a) SEM of a SWNT deposit where the catalyst was deposited through a 400 mesh TEM grid used as a mask. (b)–(d) are higher magnification SEM images corresponding to just one grid. (b) Boundary between the area with the catalyst and masked area, (c) higher magnification of the area with nanotubes in (b), (d) higher magnification of the masked area in figure (b), and (e) a TEM image showing the vertical profile of the mat.

Fig. 4 shows the ability to apply standard masking techniques to catalyst preparation. Here SWNTs were grown on a Si surface that was masked with a 400 mesh TEM grid and then had the catalyst (10 nm Al/1.0 nm Fe/0.2 nm Mo) deposited through the holes of the grid. Fig. 4b, c, and e show the dense mat of SWNTs in the open areas of the TEM grid while Fig. 4b, d show that no SWNTs grow within the area that was masked by the bars of the TEM grid. Fig. 4b also shows the boundary between the area with the catalyst and the masked area and that this boundary is very well defined. Much smaller and more intricate patterns can be developed with the application of more advanced masking and lithographic techniques for applications in field emission displays and other nanodevice development. Additionally, geometrical arrangements can also be used to deposit the catalyst onto a single face of a multisided object (such as an AFM pyramidal cantilever).

Catalyst characterization was performed on the metal underlayers using a Hitachi HD-2000. Fig. 5 shows a high-resolution TEM and X-ray line scan of the 10 nm Al/1.0 nm Fe/0.2 nm Mo formulation. The TEM image reveals that the Fe and Mo form nanometer sized particle that are distributed across the entire surface. The insert in Fig. 5a shows that the particles formed by this process are at least as small as 2 nm in diameter. Particles smaller than 2 nm are difficult to distinguish from the normal fluctuations within the pixel intensities.

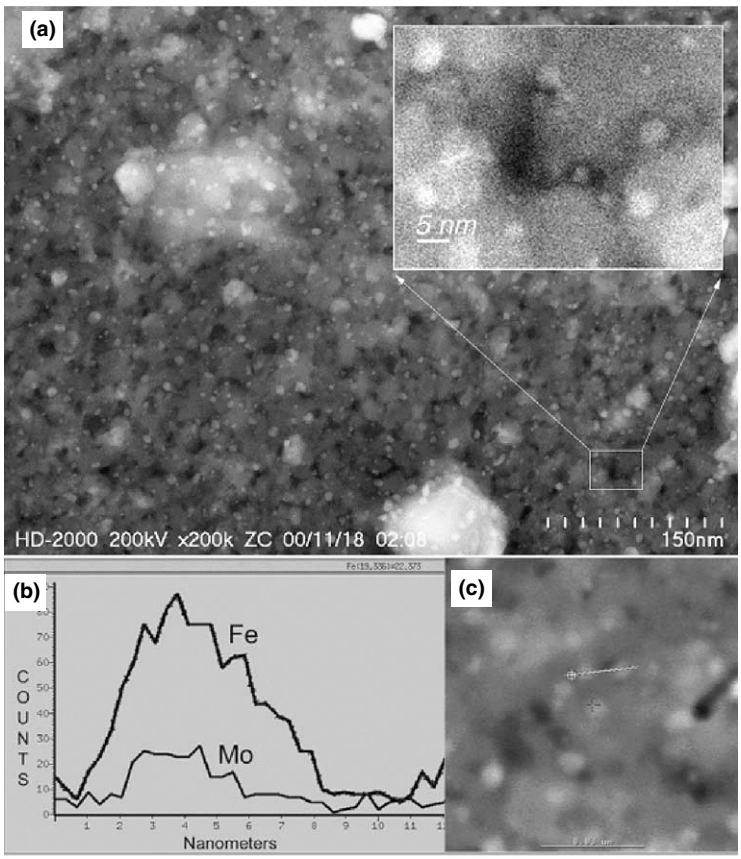

Fig. 5. (a) TEM (z-contrast mode) of the 10 nm Al/1.0 nm Fe/0.2 nm Mo catalyst formulation. The inset is an enlargement of the indicated area showing particles as small as 2 nm in diameter. The white spots are aggregations of Fe and Mo, the dark gray is the Al underlayer, and the black areas are holes through the metal film. (b) X-ray line scan of the first of two particles in (c) showing that the white particles are composed of Fe and Mo.

The X-ray line scan across these particles show that they are indeed Fe/Mo catalytic particles.

4. Conclusions

Ion beam sputtering has been used for the deposition of active catalysts and metal underlayers onto a variety of surfaces for the growth of SWNTs. The metal underlayer appears to increase the surface roughness and provide more active nucleation sites. The thickness of the catalyst layer and underlayer can be varied to produce the desired density of NTs on the surface. Shadow masking can also be applied in order to pattern the catalyst onto the surface. TEM results indicate that the active catalyst forms numerous particles on the metal underlayer with many of these particles as small as 2 nm in diameter. X-ray analysis shows that these particles are the Fe/Mo catalyst. Though most of the CVD work in the literature is about MWNTs, a theoretical study [23] suggests the amenability of CVD to grow SWNTs with small catalyst particles, availability of low carbon levels and high kinetic energy (>900 °C) which is proved by our results here. Our approach to catalyst preparation is preferable to the use of liquid based catalysts to avoid difficulties associated with restraining the catalyst to small patterned areas. This approach also works well with a variety of substrates such as silicon, SiO_2, quartz, HOPG and amorphous carbon since the metal does not seem to react with any of these surfaces. Attempts to grow nanotubes on copper surfaces with the same catalyst formulation have failed which may be due to the alloying of underlayer metals with copper. The technique presented here would be useful in certain applications wherein metallic contact between the SWNTs and the substrate is essential, for example, ohmic contact, electrical devices, sensors, and emitters.

Acknowledgements

We thank Dr. Zhenhuan Chi (Renishaw Product) and Kevin Mcilwrath (Hitachi) for vital instrumentation assistance and Richard Bormett for technical discussions.

References

[1] T. Guo, P. Nikolev, A. Thess, D.T. Colbert, R.E. Smalley, Chem. Phys. Lett. 243 (1995) 49.
[2] C.H. Kiang, W.A. Goddard, R. Beyers, D. Bethune, Carbon 33 (1995) 903.
[3] H. Dai, A.G. Rinzler, P. Nikolaev, A. Thess, D.T. Colbert, R.E. Smalley, Chem. Phys. Lett. 260 (1996) 471.
[4] J.H. Hafner, M.J. Bronikowski, B.R. Azamian, P. Nikolaev, A.G. Rinzler, D.T. Colbert, K.A. Smith, R.E. Smalley, Chem. Phys. Lett. 296 (1998) 195.
[5] P. Chen, H.B. Zhang, G.D. Lin, Q. Hong, K.R. Tsai, Carbon 35 (1997) 1495.
[6] Z.W. Pan, S.S. Xie, B.H. Chang, C.Y. Wang, L. Lu, W. Liu, W.Y. Zhou, W.Z. Li, L.X. Qian, Nature 394 (1998) 631.
[7] J. Kong, H.T. Soh, A.M. Cassell, C.F. Quate, H. Dai, Nature 395 (1998) 878.
[8] H. Kind, J.M. Bonard, L. Forro, K. Kern, K. Hernadi, L. Nilsson, L. Schlapbach, Langmuir 16 (2000) 6877.
[9] A.M. Cassell, S. Verma, L. Delzeit, M. Meyyappan, Langmuir 17 (2001) 266.
[10] A.M. Cassell, M. Meyyappan, J. Han, J. Nanoparticle Res. 2 (2000) 387.
[11] J. Li, C. Papadopoulos, J.M. Xu, M. Moskovits, Appl. Phys. Lett. 75 (1999) 367.
[12] Y.Y. Wei, G. Eres, V.I. Merkulov, D.H. Lowndes, Appl. Phys. Lett. 78 (2001) 1394.
[13] B. Kitiyanan, W.E. Alvarez, J.H. Harwell, D.E. Resasco, Chem. Phys. Lett. 317 (2000) 497.
[14] M. Su, B. Zheng, J. Liu, Chem. Phys. Lett. 322 (2000) 321.
[15] B.C. Satishkumar, A. Govindraj, R. Sen, C.N.R. Rao, Chem. Phys. Lett. 293 (1998) 47.
[16] P. Nikolaev, M.J. Bronikowsky, R.K. Bradley, F. Rohmund, D.T. Colbert, K.A. Smith, R.E. Smalley, Chem. Phys. Lett. 313 (1999) 91.
[17] Y.C. Choi, Y.M. Shin, S.C. Lim, D.J. Bae, Y.H. Lee, B.S. Lee, D.C. Chung, J. Appl. Phys. 88 (2000) 4898.
[18] R. Saito, G. Dresselhaus, M.S. Dresselhaus, Physical Properties of Carbon Nanotubes, Imperial College Press, London, 1998.
[19] A.M. Rao, E. Richter, S. Bandow, B. Chase, P.C. Eklund, K.A. Williams, S. Fang, K.R. Subbaswany, M. Menon, A. Thess, R.E. Smalley, G. Dresselhaus, M.S. Dresselhaus, Science 275 (1997) 187.
[20] A. Jorio, R. Saito, J.H. Hafner, C.M. Lieber, M. Hunter, T. McClure, G. Dresselhaus, M.S. Dresselhaus, Phys. Rev. Lett. 86 (2001) 1118.
[21] M.A. Pimenta, A. Marucci, S.A. Empedocles, M.G. Bawendi, E.B. Hanlon, A.M. Rao, P.C. Eklund, R.E. Smalley, G. Dresselhaus, M.S. Dresselhaus, Phys. Rev. B 58 (1998) 6016.
[22] R. Saito, H. Kataura, in: M.S. Dresselhaus, G. Dresselhaus, Ph. Avouris (Eds.), Topics in Applied Physics, 2001, p. 213.
[23] H. Karzow, A. Ding, Phys. Rev. B 60 (1999) 11180.